

# Preparation and Characterization of Barium Strontium Titanate $Ba_xSr_{1-x}TiO_3$ (with $x=0.6, 0.7, 0.8$ and $0.9$ ) by a Solid-State Reaction Method

A. Nagesh<sup>1</sup>, Mr. Pankaj Shende<sup>2</sup>, H. Yosief Kassahun<sup>3</sup>, P. Sreenivasulu Reddy<sup>4</sup>

<sup>1</sup>Asst.Prof. of physics,  
EIT, MAI-NEFHI, ASMARA, ERITREA Post Box No. 12676  
*nageshalakunta@gmail.com*

<sup>2</sup> Lecturer in Department of Mineral Processing Engineering,  
EIT, MAI-NEFHI, ASMARA, ERITREA Post Box No. 12676  
*yosiefkh@yahoo.com*

<sup>3</sup> Kassahun Lecturer in Physics,  
EIT, MAI-NEFHI, ASMARA, ERITREA Post Box No.12676  
*pankaishende@gmail.com*

<sup>4</sup> Asst. Professor in Physics,  
Chaitanya Bharathi Institute of Technology, Pallavolu (V), Proddatur, A.P, India.  
*palleti223@gmail.com*

**Abstract:**  $Ba_xSr_{1-x}TiO_3$  solid solutions were prepared by solid-state reaction from barium carbonate, strontium carbonate and titanium dioxide raw materials. Four compositions with  $x=0.6, 0.7, 0.8$  and  $0.9$  have been investigated. The samples are characterized by X-ray diffraction (XRD), scanning electron microscopy (SEM). The perovskite type and polycrystalline structure of the BST samples were revealed by X-ray diffraction data. The morphology, grain size distribution, porous structure and elemental composition of the sintered ceramics were analyzed by using scanning electron microscopy (SEM) and energy-dispersive X-ray (EDX) microanalysis. The variation of dielectric constant and dielectric losses with frequency variation were studied at room temperature.

**Key words:** Crystal structure, SEM, Dielectric constant, dielectric loss.

## 1. Introduction

The most widely used ferroelectrics occur in the perovskite family, with possess the general formula  $ABO_3$ ; the oxidation states of A, B and O are 2+, 4+ and 2- respectively. Barium strontium titanate is also belongs to the perovskite family [1, 2]. Barium strontium titanate (BST) based ceramics are chosen because of its several industrial applications, including dynamic random access memory (DRAM) capacitor [3, 4], microwave filters, infrared detectors, and dielectric phase shifters [5-7], due to their excellent ferroelectric, dielectric, piezoelectric and pyroelectric properties Recently barium strontium titanate has attracted much attention because of its strong dielectric and linearity adjustable Curie temperature with the strontium content over a wide range [8-10].

In recent years, increasing attention has been paid to the synthesis and characterization of nanomaterials because of their novel chemical and physical properties arising from the large surface-volume ratios and also the quantum size

effect, compared with those of bulk counterparts [11-15]; similarly barium strontium titanate ( $Ba_xSr_{1-x}TiO_3$ ) ferroelectric materials have attracted considerable attentions due to their chemical stability, high permittivity, high tunability and low dielectric losses [16]. The physicochemical properties of these nanomaterials are highly sensitive to their size, shape, and composition [17]. Moreover, the temperature range in which the ferroelectric behaviour is reflected can be easily controlled by adjusting the barium-to-strontium ratio [18].

## 2. Experimental Procedure

### 2.1. Synthesis of Materials

In the present study the high purity chemicals of Barium Carbonate, Strontium Carbonate and Titanium Dioxide were used as the raw materials.  $Ba_xSr_{1-x}TiO_3$  ( $x=0.6, 0.7, 0.8$  and  $0.9$ ) ceramic samples were prepared by conventional solid state reaction technique. The powders were mixed by ball milling for 10h for uniform mixing. The mixed powders were calcined at 1100 to 1300°C for 24 h.

After calcining the samples are ballmilled for 20 h. Fine calcined powders were pressed into disc-shaped pellets at an isostatic pressure of 10 tons. No binder was used. The pellets are sintered at 1200 to 1300 °C.

### 2.2. Structural Characterization

The phase formation in the calcined powders of  $Ba_xSr_{1-x}TiO_3$  ( $x=0.6, 0.7, 0.8$  and  $0.9$ ) ceramic samples were analyzed by applying X-ray diffraction (XRD) technique at room temperature and a step scan from  $2\theta = 0^\circ$  to  $60^\circ$ .

### 2.3 Dielectric characterization

The AC parameters such as capacitance (c) and dielectric loss of the samples were measured in the frequency range 1K Hz to 1MHz using LCR meter (HIOKI 3532-50 LCR Hi Tester). The variation of dielectric constant and dielectric loss with frequency were studied by recording the parameters at room temperature.

The dielectric constant ( $\epsilon_r$ ) was calculated using the relation:

$$\epsilon_r = ct/(\epsilon_0 A)$$

Where c is the capacitance of the pellet, t the thickness of the pellet, A the area of cross section of the pellet and  $\epsilon_0$  is the permittivity of free space ( $8.854 \times 10^{-12}$  F/m).

## 3. Results and discussion

### 3.1. XRD studies of BST ceramics

The powder XRD [19] pattern of calcined powders of  $Ba_xSr_{1-x}TiO_3$  ( $x=0.6, 0.7, 0.8$  and  $0.9$ ) ceramic samples are shown in Figure 1. Variation of Lattice parameter with composition of x is shown in figure 2.

The XRD plots of  $Ba_xSr_{1-x}TiO_3$  ( $x=0$  to 1) ceramics. For  $x=0.6, 0.7, 0.8$  and  $0.9$  compositions of  $Ba_xSr_{1-x}TiO_3$ , the maximum intensity peaks appeared at the diffraction angles  $2\theta = 31.7^\circ, 31.69^\circ, 31.67^\circ$  and  $31.60^\circ$  respectively. The composition of the barium is varied from 0.6 to 0.9, the Maximum intensity peak shifted towards the lower diffraction angles from  $2\theta=31.7^\circ$  to  $31.60^\circ$ . The lattice parameters increases linearly with increase of Ba content because of entry of the larger  $Ba^{2+}$  cation at the A site results in a regular increase of the unit-cell parameters and unit-cell volume with increasing barium content. The structure of the  $Ba_xSr_{1-x}TiO_3$  is changed from cubic to tetragonal when  $x \geq 0.7$ .

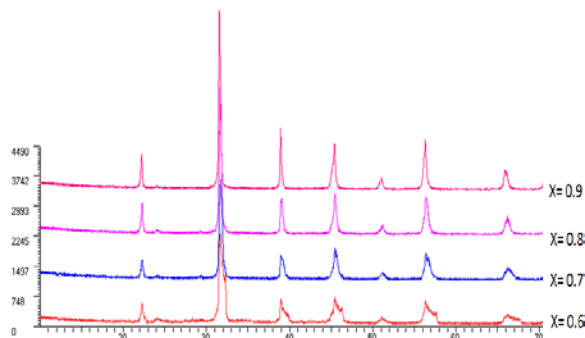


Figure 1: XRD Pattern of  $Ba_xSr_{1-x}TiO_3$  for  $x = 0.6, 0.7, 0.8$  and  $0.9$

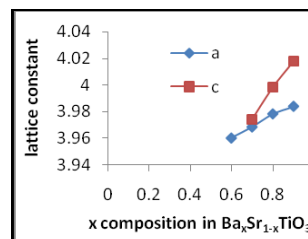


Figure 2: Lattice Constant Variation of  $Ba_xSr_{1-x}TiO_3$

### 3.2. Microstructure studies of $Ba_xSr_{1-x}TiO_3$ ( $x=0.6, 0.7, 0.8$ and $0.9$ ) ceramics

Fig. 3 represents the scanning electron micrograph of  $Ba_xSr_{1-x}TiO_3$  ( $x=0.6, 0.7, 0.8$  and  $0.9$ ) ceramics. The materials average grain size was determined directly from the SEM micrographs by using the linear interception method. The grain size of a ceramic material is a critical microstructure feature. The grain size in piezoelectric materials depends on the material composition and the sintering process. The samples with heterogeneous grains are having the grain sizes in the range of 2 to 4  $\mu m$ . The Energy dispersive analysis [20, 21] of X-ray of  $Ba_xSr_{1-x}TiO_3$  ( $x=0.6, 0.7, 0.8$  and  $0.9$ ) is shown in figure 4.

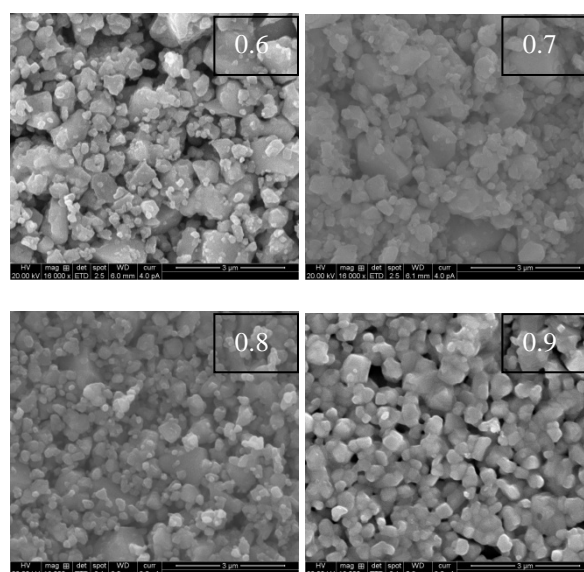


Figure 3: Scanning Electron Micrographs of  $Ba_xSr_{1-x}TiO_3$  ( $x=0.6, 0.7, 0.8$  and  $0.9$ )

0.6

0.7

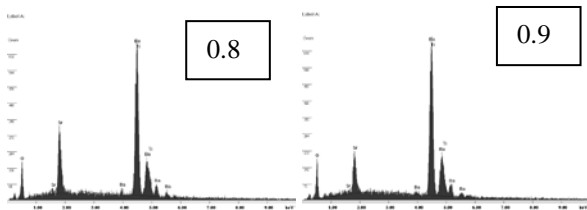
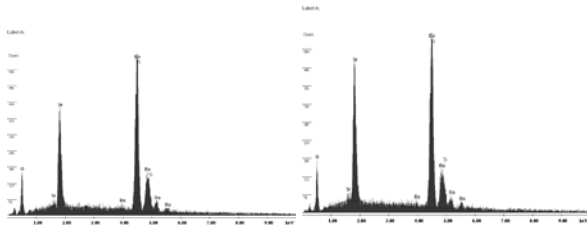


Figure 4. EDAX plot of  $Ba_xSr_{1-x}TiO_3$  ( $x=0.6, 0.7, 0.8$  and  $0.9$ ) ceramics

### 3.3. Dielectric constant and dielectric loss

The variation of dielectric constant of  $Ba_xSr_{1-x}TiO_3$  ( $x=0.6, 0.7, 0.8$  and  $0.9$ ) with frequency variation at room temperature is shown in Fig. 5. The variation of dielectric constant is remains constant for  $x= 0.7$  composition. The variation of dielectric loss of  $Ba_xSr_{1-x}TiO_3$  ( $x=0.6, 0.7, 0.8$  and  $0.9$ ) with frequency variation at room temperature is shown in Fig. 6

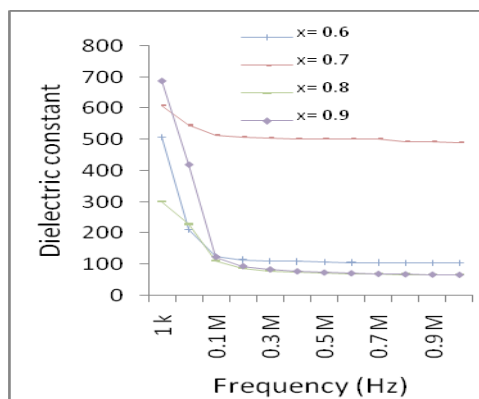


Figure 5 Variation of dielectric constant with frequency for  $Ba_xSr_{1-x}TiO_3$  ( $x=0.6$  to  $0.9$ ) at room temperature.

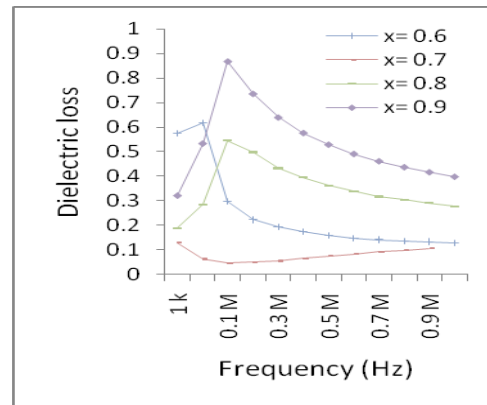


Figure 6 Variation of dielectric loss with frequency for  $Ba_xSr_{1-x}TiO_3$  ( $x=0.6-0.9$ ) at room temperature.

## 4. Conclusions

The result of lattice parameter measurements and XRD patterns conforms the perovskite phase transformation of the  $Ba_xSr_{1-x}TiO_3$ ,  $x = 0.6, 0.7, 0.8$  and  $0.9$  system. The unit cell volume was observed to increase slightly at higher  $x$  ratios. The lattice parameter of the unit cell was also observed to increase slightly with increasing  $x$ . The structure of the  $Ba_xSr_{1-x}TiO_3$  is changed from cubic to tetragonal when  $x \geq 0.7$

## References

- [1]. N. Setter, Electroceramics: looking ahead, *J. Eur. Ceram. Soc.* 21 (2001) 1279-1293.
- [2]. N.W. Thomas, A new framework for understanding relaxor ferroelectrics, *J. Phys. Chem. Solids* 51 (12) (1990) 1419-1431.
- [3]. Scott, J. F., High-dielectric constant thin films for dynamic random access memories. *Ann. Rev. Mat. Sci.*, 1998, 28, 79–100.
- [4]. Takasu, H., The ferroelectric memory and its applications. *J. Electroceram.*, 2000, 4, 327–338.
- [5]. Verbitskaja, T. N., *Variconds*. Gosenergoizdat, Moscow-Leningrad; 1958 [in Russian].
- [6]. Vendik, O. G., ed., *Ferroelectrics in microwave engineering*. Sov. Radio, Moscow, 1979 [in Russian].
- [7]. Chang, W. and Sengupta, L. C., MgO-mixed  $Ba_{0.6}Sr_{0.4}TiO_3$  bulk ceramics and thin films for tunable microwave applications. *J Appl Phys*, 2002, 92, 3941–3946.
- [8]. Q. Xu, X.F. Zhang, Y.H. Huang, W. Chen, H.X. Liu, M. Chen, B.H. Kim, Effect of MgO on structure and nonlinear dielectric-properties of  $Ba_{0.6}Sr_{0.4}TiO_3$ /MgO composite ceramics prepared from superfine powders, *J. Alloys Compd.* 488 (2009) 448-453.

- [9]. Li-na Su, Peng Liu, Ying He, Jian-ping Zhou, Lei Cao, Cheng Liu, Huai-wu Zhang, Electrical and Magnetic Properties of low temperature sintered  $x\text{Ba}_{0.6}\text{Sr}_{0.4+(1-z)}\text{Ni}_{0.2}\text{Cu}_{0.2}\text{Zn}_{0.62}\text{O}(\text{Fe}_2\text{O}_3)_8$  composite ceramics. *J. Alloys Compd.* 494 (2010) 330-335
- [10]. Gulwade, Devidas; Gopalan, Prakash, Diffuse phase transition in La and Ga doped barium titanate, *Solid State Commun.* 146 (2008) 340-344.
- [11]. Chang Q. Sun, (2007), Size dependence of nanostructures: Impact of bond order deficiency *Progress in Solid State Chemistry*, 35: 1-159.
- [12]. A.P. Alivisatos, (1996), Semiconductor clusters, nanocrystals and quantum dots, *Science*, 271: 933-937.
- [13]. J. Hu, T.W. Odom, C.M. Lieber, (1999), Chemistry and Physics in One Dimension: Synthesis and Properties of Nanowires and Nanotubes , *Acc. Chem. Res.* 32 : 435-445.
- [14]. L.E. Brus, J.K. Trautman, Nanocrystals and Nano-Optics, *Philos. Trans. R. Soc. London Ser. (1995) , A-Math Phys. Eng. Sci.* 353: 313-321.
- [15]. J.R. Heath, (1999), Nanoscale Materials, *Acc. Chem. Res.* 32: 388.
- [16]. Ming-li Li, Hui Liang, Ming-xia Xu, (2008), Simple oxalate precursor route for the preparation of brain-like shaped barium–strontium titanate:  $\text{Ba}_{0.6}\text{Sr}_{0.4}\text{TiO}_3$ , *Mater. Chem. Phys.* 112: 337-341.
- [17]. Xiao W, Gang X, Zhaohui R, Yonggang W, Ge S, Gaorong H, (2008), Composition and shape control of single-crystalline  $\text{Ba}_{1-x}\text{Sr}_x\text{TiO}_3$  ( $x = 0-1$ ) nanocrystals via a solvothermal route, *J. Crystal Growth*, 310 : 4132-4137.
- [18]. T. Mazon, M.A. Zaghete, J.A. Varela , E. Longo, (2007), Barium strontium titanate nanocrystalline thin films prepared by soft chemical method, *J. Euro. Ceram. Soc.* 27: 3799-3802.
- [19]. Charles S. Barrett, jerome B. Cohen, John Faber, Jr., Ron Jenkins, Donald E. Leyden, John C. Russ and Paul K. Predecki, *Advances in X-ray Analysis*, Springer (1986)
- [20]. DC Bell and AJ Garratt-Reed, *Energy Dispersive X-ray Analysis in the Electron Microscope (Microscopy Handbooks)*, Springer (2003),
- [21]. John C. Russ, *Fundamentals of energy dispersive x-ray analysis*, Springer (2005)